Metallurgical and Materials Engineering *Scientific paper*
Association of Metallurgical Engineers of Serbia AMES *DOI: 10.30544/244363*

ON THE ROLE OF APPLYING GROOVE PRESSING TECHNIQUE BEFORE FRICTION STIR PROCESSING OF COPPER: MICROSTRUCTURAL AND MECHANICAL EVALUATION

*Mohsen Barmouz[1, *], Abbas Dodangeh[2], Hadi Ghiabakloo[2], Kaveh Rahimi Mamaghani[2]*

[1]Young Researchers and Elite Club, Zanjan Branch, Islamic Azad University, Zanjan, Iran
[2]Department of Materials Science and Engineering, Sharif University of Technology, Azadi Avenue, Tehran, Iran

Received 14.10.2017
Accepted 29.12.2017

Abstract

The effect of prior constrained groove pressing on friction stir processing (FSP) of pure copper was investigated. The results illustrate the development of high strain and strength of FSP samples along with an increased strength base metal as a result of applying for a prior constrained groove pressing (CGP) pass. The influences of further FSP passes on the microstructures, and mechanical properties were also shown. The microstructural evaluation of the specimens indicated up to 10 times grain size reduction in FSP specimens as well as equiaxed microstructural morphology. Mechanical properties of the specimens were carried out through tensile and microhardness tests. It was demonstrated that the FSP could improve the strength and ductility of the specimens simultaneously through improved mechanical properties of the base metal resulting from prior CGP. The performed calculations show that values of dislocation density of the CGPed specimens experienced significant change after applying for FSP passes.

Keywords: *Microstructural and mechanical characterization; X-ray diffraction; Grain refinement; Dislocations; Constrained groove pressing; Friction stir processing.*

Introduction

Nano-crystalline materials are generally produced by two different methods named bottom-up and top-down. In the case of the former, the nanostructured materials are formed atom-by-atom or layer-by-layer. However, in the case of the latter, the

[*] Corresponding author: Mohsen Barmouz, *Mbarmouz@ut.ac.ir*

technique to produce a nanocrystalline structure is severe plastic deformation (SPD) [1-3].

When the severe plastic deformation is applied to the material - dislocation density is increased in the deformed material, and dense dislocation walls formed are converted into the high-angle grain boundaries. Materials produced via this method typically possess superior mechanical properties such as increased strength, ductility, toughness, and superplasticity at higher strain rates and low temperatures relative to the bulk material from which they were produced [2].

Several SPD methods, such as equal channel angular pressing (ECAP), multi-directional forging (MDF), constrained groove pressing (CGP), accumulative roll bonding (ARB) and high-pressure torsion (HPT), have been used to impose intense strain into the bulk materials [4-11].

CGP was first developed by *Shin et al*. [12] in which samples were subjected to plane strain deformation by alternating pressing using by both asymmetrically grooved and constrained flat dies. The gap between the upper and lower dies was equal to the thickness of the sheet. Upon repetitive applications of this method, intense plastic strain accumulates within the sample, and an ultrafine grain structure was achieved without any changes in the sample dimensions [2, 12, 13].

Mechanical properties of the materials processed by CGP are comparable with those of materials processed by other techniques applying intense plastic strain. It was indicated that in the CGP process, deformation is not uniform throughout the thickness and the effective strain, at the center of the sample, is higher than that on the surface of the sample. However, it is notable that with increasing the number of CGP passes, this non-uniformity becomes negligible [14].

Various methods have been developed for improvement of poor ductility of the ultra-fine grained and nanostructured materials [15]. One of the most applicable methods is friction stir processing (FSP) [16].

FSP is a new thermo-mechanical process developed on the basis of the friction stir welding (FSW). This technique is used for modifying the microstructure of metals, surface composites production, homogenizing the nano-phase aluminum alloys, and refinement of the microstructure of the cast aluminum alloys [17-20]. Additionally, this process is energy efficient, versatile and environmentally appropriate [17].

Heat generation in FSP results from the frictional contact between the tool and the work-piece and with plastic deformation of the work-piece. Increase in the local temperature of the sample causes material softening around the pin, and the combination of the traverse and rotational movements leads to material flow from the front to the back of the pin [17].

It has been demonstrated that different regions appearing in the friction stir processed (FSPed) sample exhibit various mechanical properties because of their different grain and precipitation sizes and non-uniform distribution [17].

There are several investigations on the effect of FSP on microstructure and mechanical properties of pure copper in the literature. *Su et al.* [18] achieved a nanostructured copper (with grain sizes between 50 to 300 nm) via a single pass FSP. They used tools with small shoulder sizes together with rapid cooling of the sample during the process. *Xue et al.* [16] showed that the strain hardening capacity of the FSPed copper is higher than those of ECAPed samples. They found that in the case of FSPed copper, grains are equiaxed and most of the grain boundaries are sharp, clear and

approximately straight resulting in the grain boundaries with high angle misorientation. Recently, FSW of the CGPed or ARBed aluminum alloys sheets has received lots of attention [21-23]. This is due to the fact that ultra-fine grained materials cannot be made in large size for industrial applications which is the consequence of limitations in the SPD process such as the load capacity and rigidity of the equipment [21-23].

To the best of our knowledge, there is no report on the investigation of the microstructure and mechanical properties of the CGPed copper followed by various FSP passes in the literature. Thus, the aim of this research was to characterize the possible effects of applying various passes of FSP on microstructure and mechanical properties of both CGPed pure copper and the reference pure copper. As it is known the FSPed specimens in spite of good strength and ductility in stir zone, suffer from low strength in the base metal.

Experimental

In the present study, fully annealed (at 750ºC for 3h and then cooled in the furnace) pure copper (99.99%) sheets with dimensions of 84mm×60mm×3mm were used to study the effects of CGP on grain refining and strengthening of copper sheets at room temperature. In the first stage of CGP, the sheet was pressed via placing the copper sample between the upper and lower grooved dies. In the second stage, the grooved sheet was flattened with the flat dies. After 180° rotation of specimen around the sheet perpendicular axis, further groove pressing and finally utilization of flat dies caused a relatively uniform distribution of plastic strain (one pass CGP) throughout the specimen [21,24, 25]. It should be noted that the width of corrugating dents of grooving dies was equal to the sheet thickness which reveals pure shear deformation condition throughout the process. In this study, Teflon layers between the copper sheet and dies were used as a lubricant. The pressing force of process was supplied by using a 100-ton hydraulic pressing machine at a ram speed of 2.5 mm/min. In this research, samples were subjected to CGP process only for one pass with 0.16% applied strains.

In this research, based on the previous studies, the optimum rotational and traverse speeds which resulted in an intense grain size reduction were 700 rpm and 80 mm/min, respectively [26]. The processing tool was tilted at an angle of 2°. FSP tool was made of hot-working steel with the shoulder diameter, pin diameter and length of 9, 4 and 2 mm, respectively. The specimens were clamped onto thick St37 steel, and the specimens were fixed by the bolts. In the current work, annealed specimens were subjected to the multi-pass FSP with and without prior CGP. The list and codes of prepared samples are reported in Table 1.

Table 1. List of processed specimens.

List of Specimens	Specimens' Description
1C	1-pass CGPed specimen
1C-1F	1-pass CGPed and then 1-pass FSPed specimen
1C-2F	1-pass CGPed and then 2-pass FSPed specimen
1F	1-pass FSPed specimen
2F	2-pass FSPed specimen

Microstructural changes, from base metal to the stirred zone, were examined by optical microscopy (OM) and field emission scanning electron microscopy (FESEM) and the grain size was calculated using linear intercept method.

All samples surfaces were prepared by standard metallographic techniques and etched with a solution of 100 ml distilled water, 15 ml H_2O_2 and 2.5 g $FeCl_3$.

Microhardness properties of the specimens were measured on the cross-section of the welds and perpendicular to the processing direction in depth of 1 mm from the FSPed surface using a 30 g load for 15 s.

Tensile tests of the annealed pure copper and the examined specimens were determined at ambient temperature via tensile machine at the strain rate of 10^{-1} mm s^{-1}. Three tensile specimens were machined from each sample. It should be noted that the tensile specimens were prepared according to the ASTM E8M (with 25.4 mm bar) and cut from the stir zone in the longitudinal direction of FSPed specimens.

Wide angle X-ray scattering (WAXS) analysis was performed using an X-ray diffractometer operating at 40 kV and 30 mA for Cu Kα radiation (λ=0.154 nm). XRD scans were performed on the cross-sections of the specimens and perpendicular to the FSP direction. The X-ray patterns were obtained in the range of 10° - 110° and in the step widths of 0.02°.

Results and discussion

Microstructural evolution

Fig. 1(a) shows the microstructure of annealed pure copper. The microstructure of this sample after applying one pass of CGP is shown in Fig. 1(b) which indicates the grain size reduction (up to 50 μm) due to the CGP when compared to that of annealed one. This is due to the fact that in the SPDed materials, the coarse-grained microstructure is changed to cell blocks and dislocation cells which lead to grain refinement [21].

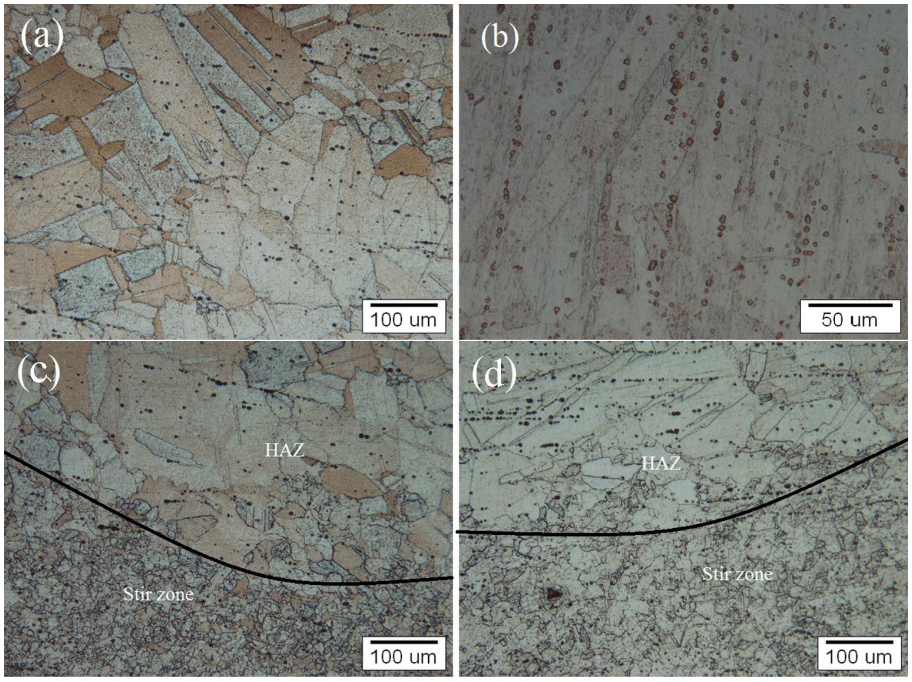

Fig. 1. Optical microscopy images of the (a) and (b) base metal of annealed pure copper, and 1C, respectively and (c) and (d) the HAZ and stir zone in the 1F and 2F, respectively.

Figs. 1(c) and 1(d) show the micrograph images of 1F and 2F, respectively. The microstructures of these samples show three different zones including stir zone, heat affected zone (HAZ) and base metal. It has been reported in previous researches [16] that FSPed aluminum alloys exhibit four zones: base metal, stir zone with fine recrystallized grains, TMAZ with coarse deformed grains and HAZ with equiaxed grains coarser than those for the base metal. These regions possess various mechanical properties owing to the different grain and precipitation sizes and corresponding size distribution [17].

Fig. 1c and d, show that there is no distinct TMAZ in the FSP processed copper as also reported in ref. [27]. This phenomenon can be attributed to the high thermal conductivity of the copper compared to other metals such as aluminum.

Stir Zone (SZ):

Fig. 2 shows the microstructures of the stir zones of 1F (Fig. 2(a)) and 2F (Fig. 2(b)). Due to the intense plastic deformation and high-temperature exposure within this zone during FSP, recrystallized fine grains appear in the stir zone of FSPed samples. In this region, fine equiaxed grains with a large fraction of high angle grain boundaries are formed as a result of dynamic recrystallization during FSP of copper which contains relatively low stacking fault energy (SFE) [28,29]. This phenomenon leads to the formation of the new nucleus within the processed zone which causes hindrance to grain growth. FSP parameters including tool geometry, work-piece composition, work-piece temperature, active cooling and vertical pressure affect the peak temperature of the

thermo-mechanical cycle during FSP which is a significant factor in determining the recrystallized grain size of the stir zone [16, 17]. Dynamic recrystallization is a dominant factor in controlling the grain size of FSPed materials. As it is seen in the microstructural images indicated in Fig. 2, the grain sizes of the FSPed specimens show a considerable reduction as compared with that of the annealed one.

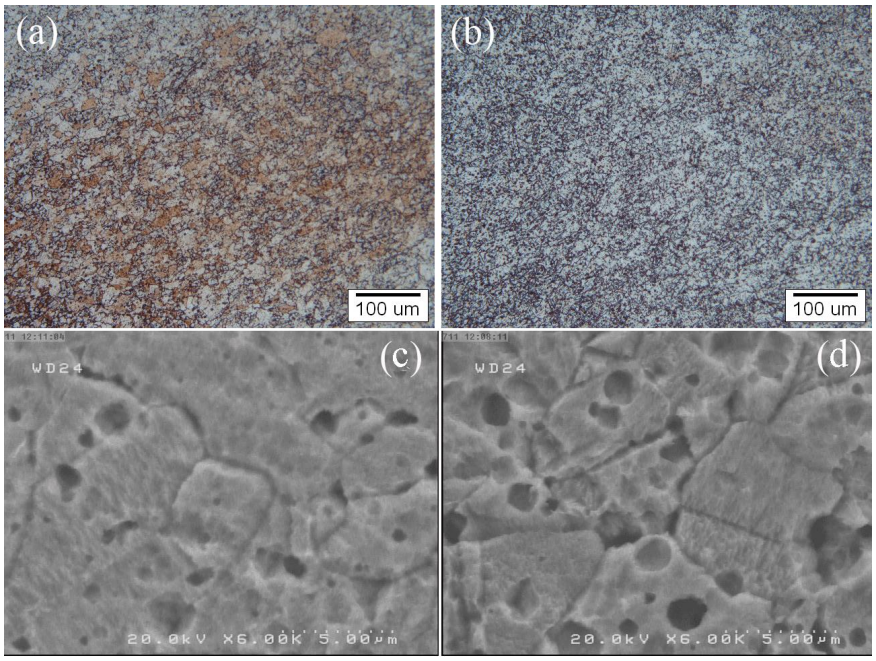

Fig. 2. Optical microscopy images of the stir zone in the (a) 1F and (b) 2F, and SEM images of the stir zone in the (a) 1F and (b) 2F.

SEM micrographs of stir zone in 1F and 2F are shown in Fig. 2c and d. The grain size of this region for 1F and 2F, after one and two passes of FSP, is about 12.3 and 6 µm, respectively. It could be seen that an increase in the FSP pass number causes a tangible reduction in the grain size in the stir zone of the annealed sample. This could be attributed to the higher strain which is imposed to the stir zone upon two FSP passes leading to more severe dynamic recrystallization. This phenomenon could also be attributed to higher grain boundary density after the first pass of FSP which they act as new nucleation sites in the second FSP pass.

Microstructures of the HAZ for the 1F and 2F are illustrated in Fig. 1c and d. Due to the heat generation resulting from FSP, equiaxed grains of the HAZ start to grow [17, 30]. Thus, as can be seen, the grain size of the HAZ is slightly higher than that of the base metal (see Fig. 1(a)).

Fig. 3 shows the microstructures of the 1C-1F and 1C-2F samples. Stir, and HAZ zones are shown in this figure indicating the formation of no distinct TMAZ. This phenomenon could be used in order to explain that the initial constrained groove pressing has no effect on the formation of the TMAZ for FSPed samples.

Microstructures of the HAZ for 1C-1F and 1C-2F are shown in Fig. 3. In Fig. 3(a), in consequence of the initial deformation with CGP, some recrystallized grains can be seen in the HAZ that includes coarsened grains. These recrystallized grains in the HAZ have a strong effect on mechanical properties of this region [21]. On the other hand, in the sample subjected to the two FSP passes after CGP (Fig. 3(b)), only heat input-induced grain growth is detectable in the HAZ. Additionally, in some regions of HAZ in the CGPed samples and after FSP, due to abnormal growth, the grain sizes are not uniform [31].

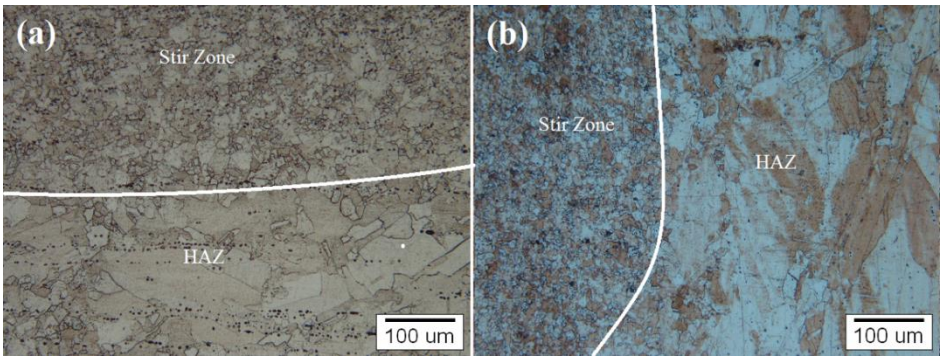

Fig. 3. Optical microscopy images of the HAZ and stir zone in the (a) 1C-1F and (b) 1C-2F.

Microstructures of the stir zones for the1C-1F and 1C-2F samples are shown in Fig. 4. As a result of the mechanisms mentioned above (dynamic recrystallization), fine recrystallized grains appear in the stir zone of these samples which are finer than those of the base metal (see Fig. 1 (b)).

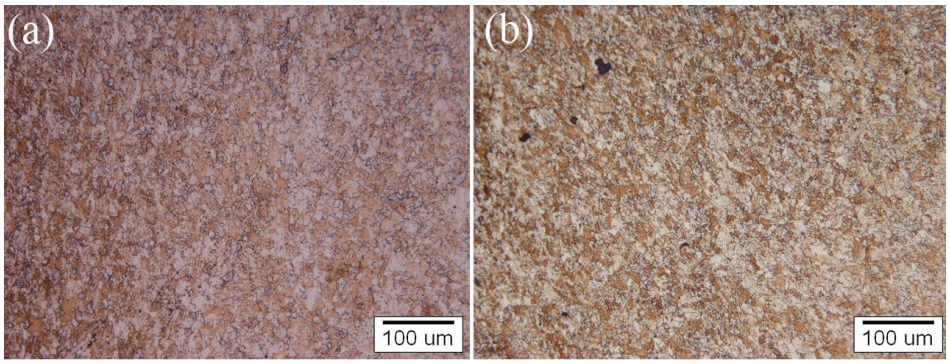

Fig. 4. Optical microscopy images of the stir zone in the (a) 1C-1F (b) 1C-2F.

In order to investigate the effects of the initial deformation (one pass CGP) and number of FSP passes on the grain size of the stir zone, SEM micrographs of 1C-1F and 1C-2F samples are displayed in Fig. 5.

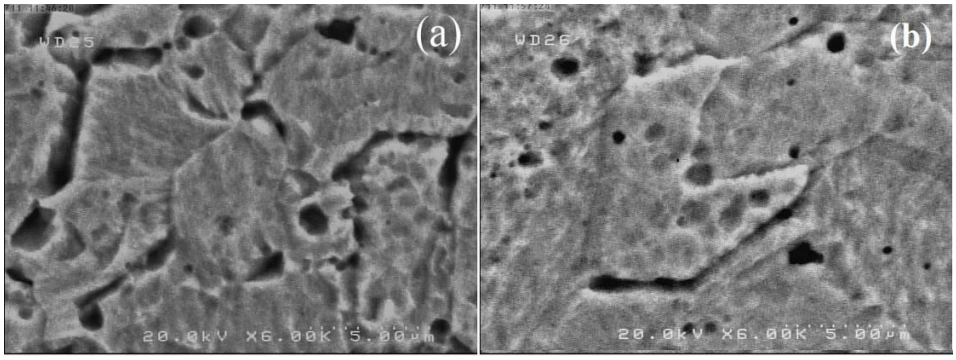

Fig. 5. SEM images of the stir zone in the (a) 1C-1F (b) 1C-2F.

It is found that the stir zones of the 1C-1F and 1C-2F exhibit grain sizes of up to 8.6 and 11.3 µm, respectively. The results show that the stored strain in the base metal, due to the CGP, affects the evolution of microstructure in the stir zone during FSP. In the CGPed sample, initial deformation (1 pass CGP) causes the formation of appropriate nucleation sites for recrystallization. Unlike the FSPed specimens without prior CGP, upon increasing the FSP passes on the CGPed sample; the grain growth occurs owing to increase of the heat input. This phenomenon may be attributed to the fact that, in the case of 1C-1F, recrystallization of the stir zone becomes saturated and with increasing the FSP passes no more grain refinement occurs in the sample in this zone. By comparing the microstructures of all the samples mentioned above, it can be seen that; the initial deformation (one pass CGP) has some effects on the microstructure of the FSPed samples, both in stir zone and HAZ, because of the formation of statically recrystallized grains in HAZ.

X-ray profile analysis

X-ray profile analysis is a well-known method which provides some important data on the structure of materials processed by SPD methods. The microstructural evolution, at different stages of the deformation process, was followed by XRD. Fig. 6 shows XRD profiles of the examined specimens.

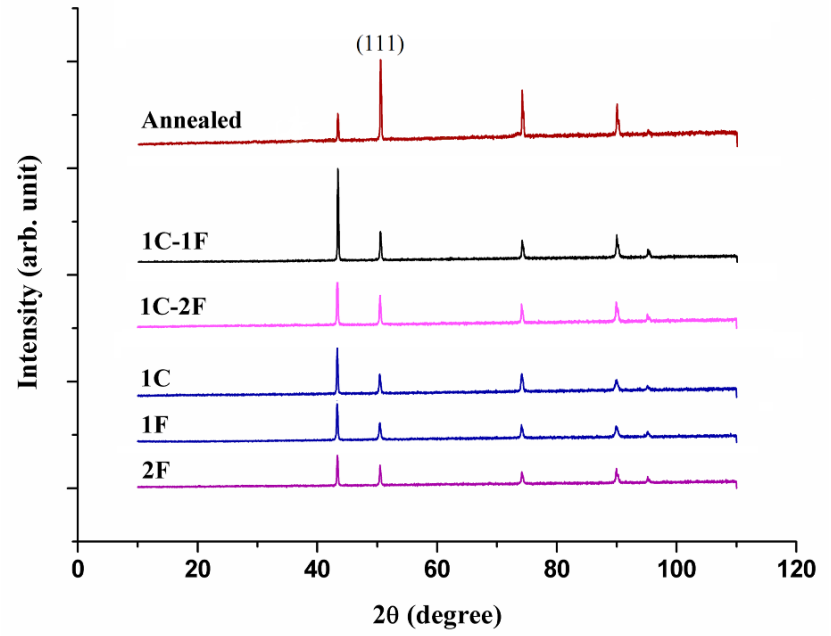

Fig. 6. XRD profiles of annealed and processed specimens.

Resolving full-width at half-maximum (FWHM) for (111) peak was carried out, and the results are shown in Table 2. It is known that the analysis of X-ray peaks broadening can provide information on crystallite size in polycrystalline materials. It is known, the number of strain increases by increasing in the FWHM. Based on the Scherrer formula, increase in FWHM indicates the reduction of crystallite sizes [32]. It is worth mentioning that the broadening of (111) peak at different processes is in conformity with the grain size variations which were calculated for the specimens through the SPDs mentioned in the previous section.

Table 2. List the FWHM value of (111) peak for annealed and processed specimens.

Specimens	FWHM in (111)
Annealed	0.0787
1C	0.11
1C-1F	0.1574
1C-2F	0.1378
1F	0.12
2F	0.1968

Tensile properties

Fig. 7 shows the true stress-strain curves for the specimens. As it is seen, the processed specimens have tangible differences in tensile properties which could mainly be originated from their different microstructural, heat cycle and mechanical stress history. It is indicated that the yield stress of 1C specimen is up to 5 times higher than that of the annealed one. This resulted from the smaller grain size and also the higher content of dislocation density formed by applied severe mechanical stresses.

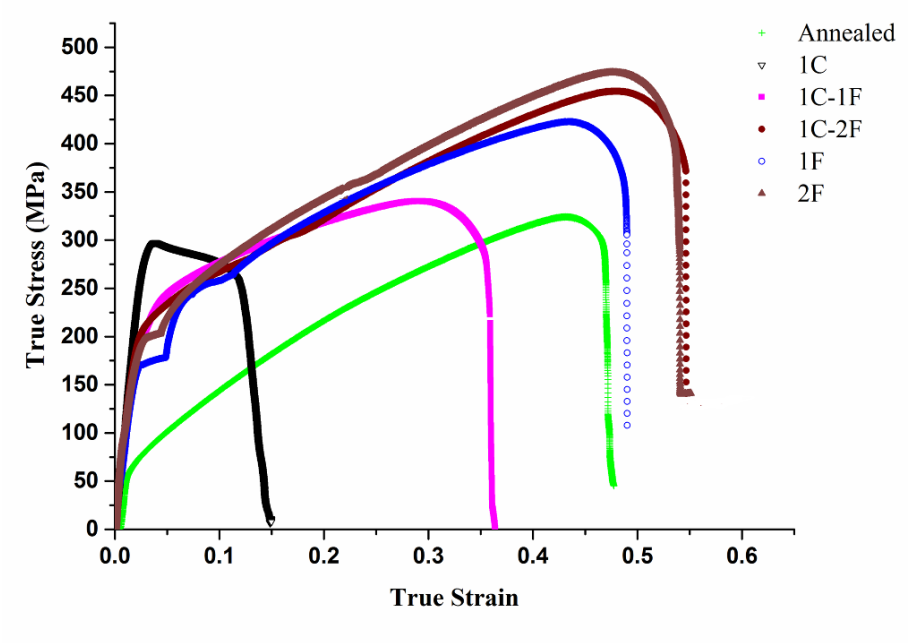

Fig. 7. True stress-strain curves of the annealed and processed specimens.

The trend of yield stress variation in the examined samples is shown in Fig. 8. The increase of the yield stresses is diminished for the specimens FSPed after CGP (1C-1F and 1C-2F) as compared to that of 1C, although they are still notably higher than that of the annealed one. Grain size reduction in these specimens as compared to those of annealed ones is the most probable reason for this phenomenon leading to high resistance of dislocations to slide and material to flow.

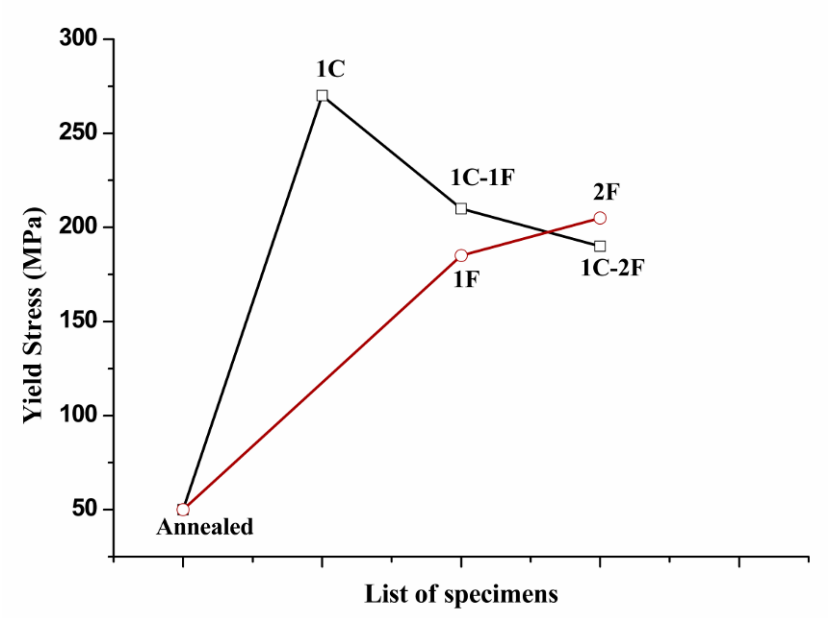

Fig. 8. The yield stress of the annealed and processed specimens.

As discussed earlier in the microstructural section, applying SPD on the specimens leads to the formation of fine grains with high angle grain boundaries which both are positive factors in the enhancement of yield stress. As mentioned before, the FSPed specimens benefited from higher heat input as compared to the CGPed ones. The high heat input in the FSPed specimens, after CGP, softens the material by formation of dynamically recrystallized equiaxed grains which facilitate the material flow initiation. As a result, FSP reduces the yield stress in the CGPed specimens.

In the case of 1F and 2F, the yield stresses show a notable enhancement (measured to be about 260% and 320%) higher than that of the annealed specimen as a consequence of the previously mentioned reasons for 1C-1F to 1C-2F. Also, the yield stress reduction in 1C-2F compared to that of 1C-1F stands for the higher heat input in former one which reduces the dislocation density resulting from 1-pass CGP. Due to its smaller grain size and higher dislocation density, the yield stress of 1C-1F is higher than that of 1F. The yield stress of 2F and 1F is nearly equal to 1C-1F and 1C-2F, respectively; which is as a result of similar microstructural characteristics.

As it is reported in many researches, the dislocation density plays a vital role in controlling the mechanical properties of the metals. Thus, the dislocation density variation of the SPDed material could act as an important factor in the explanation of their tensile properties. Bow-up model was used for calculation of the dislocation densities of the examined specimens. Based on this model, the yield would be initiated if the dislocation configuration reaches the semicircle, and its critical stress is calculated by the following equation [11]:

$$\tau_{critical} = \frac{Gb}{2\pi(1-\upsilon)}\left[\left(1-\frac{3\upsilon}{2}\right)\ln\left(\frac{L}{b}\right)-1+\frac{\upsilon}{2}\right] \quad 1$$

where: G is the shear modulus, b is the burgers vector, ν is the poison's ratio and L is the average dislocation length. For the grain sizes larger than 100 nm, L is equal to $\rho^{-\frac{1}{2}}$ where ρ is the dislocation density value [11, 33]. The yield stress of the fine-grained materials can be expressed as:

$$\sigma_{ys} = \sigma_0 + M\tau_{critical} \quad 2$$

where: σ_0 is the frictional stress equals to 5 MPa [34], and M is the Taylor Factor equals to 3.06 for copper. For calculation of dislocation density by subtracting Equation 1 from Equation 2, G was replaced by the third of the elastic region slope for each specimen's tensile curve. Moreover, the *b* and *ν* values were chosen to be 25×10^{-10} m and 0.34, respectively [20].

The different yield stress values were replaced from the Fig. 8 in the Equation 1. Fig. 9 shows the calculated dislocation density values for different specimens. According to this figure, the dislocation density of the 1C considerably increases from 4.3×10^{13} in the annealed specimen to 5.9×10^{14}, which was expected because of intense mechanical stresses and high strain values applied to the specimens through the SPD [11]. This severe deformation in the material leads to the formation of cell walls resulting in higher dislocation density. However, Fig. 9 shows that the dislocation density values decrease with applying the FSP passes on the 1C. It is due to the fact that higher amount of input heat together with dynamic recrystallization during FSP annihilate the dislocations. According to this figure, 1C-2F shows a notable increase in dislocation densities rather than that of 1C-1F. This result could be attributed to the governing effect of severe mechanical stresses applied to the specimens through the two FSP passes. *Barmouz et al*. [20] reported that applying two FSP passes on pure copper could reduce the dislocation density. However, the shoulder of the tool used in their experiment had the diameter larger than in the current work which caused a higher heat input inside the specimen.

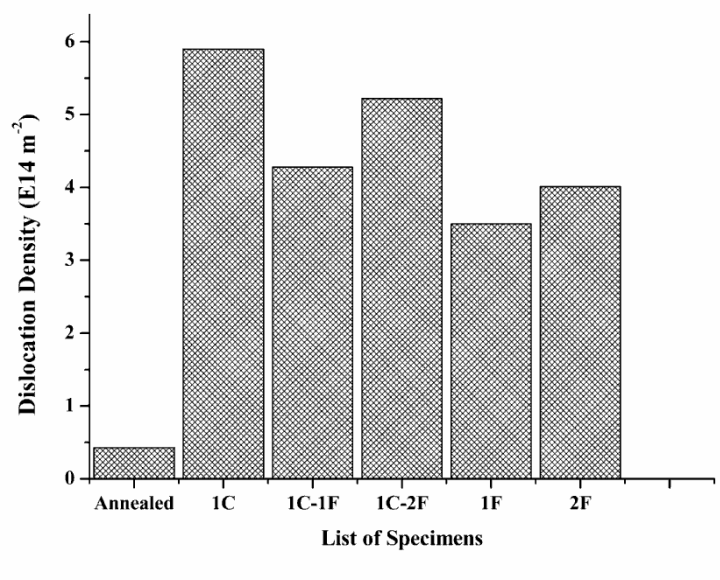

Fig. 9. Dislocation density values of the annealed and processed specimens.

As it is shown in Fig. 9, 1F and 2F have larger dislocation density values in comparison with that of the annealed specimen. This phenomenon happened as a result of the severe reduction of grain size and formation of new nucleation sites triggering dislocations formation.

Fig. 9 also shows that the specimens experiencing only one and two FSP passes contain lower values of dislocation densities compared to those of CGPed prior to FSP. This phenomenon could be explained by the fact that, in the specimens pre-processed by CGP, the higher amount of mechanical stress leads to the formation of a high amount of low angle grain boundaries with misoriented walls which can weaken the role of FSP in dislocation elimination. Dislocation densities increase in 2F rather than 1F could be due to the smaller grain size and more intense stress in the former one, which has a governing role versus the higher experienced input heat.

The ultimate tensile strengths (UTS) of the specimens are listed in Table 3. The plastic deformation of the metals under tension can be explained by some significant factors such as dislocation density, grain size, heat cycle and grains shape. As reported in many researches, the strain hardening is one of the most important factors controlling the tensile properties of the specimens [15, 34]. It is worth mentioning that the lower amount of dislocation density leads to a higher extent of strain hardening due to the presence of larger space for dislocation gathering [15, 34]. The other important controlling factor is the input heat which participates in the material softening and thus enhancing the strain value. The shape of the grains can determine their stacking possibility through the movement.

Table 3. Annealed and processed specimens ultimate tensile strengths and strains values.

List of the specimens	Ultimate Tensile True Strength (MPa)	True Strain
Annealed	320	0.45
1C	301	0.12
1C-1F	345	0.31
1C-2F	455	0.51
1F	423	0.44
2F	474	0.50

The ultimate tensile strength results exhibited in Table 3. 1C displayed no considerable ultimate tensile strength enhancement when compared to its yield stress. The ultimate tensile strength and strain value of 1C-1F substantially increase by applying for the FSP pass after CGP. This phenomenon suggests that the intense mechanical stress together with heat input in the stir zone lead to microstructure refinement and thus a sharp reduction in dislocation density as a result of dynamic recrystallization.

In the case of 1C-2F, second heat cycle on the CGPed specimens changes the dominant factors. Indeed, it softens the metal more, makes the grains coarser and lowers the dislocation density. As a result, tangible enrichment in both of strength and strain compared to 1C-1F has been achieved.

In the case of 1F and 2F specimens, the comparable strain and strength values with 1C-2F are observed in Table 3 which might be due to their lower dislocation density compared to 1C-1F. This phenomenon causes a higher possibility of dislocation gathering which leads to a higher amount of strain hardening.

Microhardness profiles

Fig. 10 shows the microhardness profiles for the processed specimens. Regarding the microhardness value of the annealed copper, measured to be 40 HV, microhardness of the processed specimens is evidently increased. Assessment of the obtained results demonstrated that the variation in microhardness values is highly governed by dislocation densities.

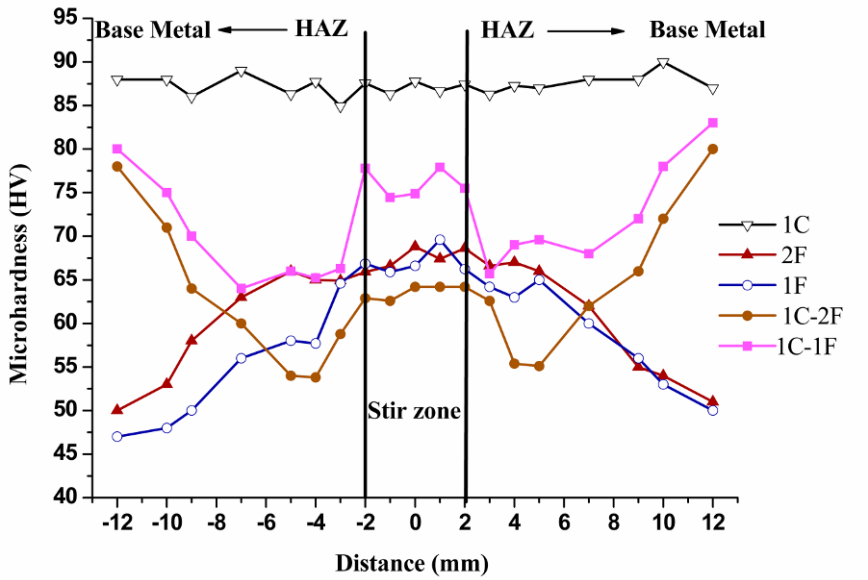

Fig. 10. Microhardness values of the processed specimens.

The CGP led to remarkable hardness enhancement of the annealed specimen which is due to the smaller grain size, a higher value of dislocation density and grain boundaries strengthening. However, as a result of applying FSP passes on CGPed specimens, a discernible reduction of hardness is observed. In the case of FSPed specimens, the lower dislocation density and high heat input weaken the dislocation role in grain boundaries strengthening, and thus the microhardness values tend to be lessened.

In the case of 1C-1F and 1C-2F, the microhardness values in HAZ are reduced in comparison with stir zone as a result of average coarser grain sizes in HAZ, while they show an incremental trend to the base metal which has been work hardened after CGP. In 1F and 2F, the microhardness values of the base metal are dramatically lower than those specimens processed by CGP prior to FSP.

Conclusions

Experimental investigations were carried out to evaluate prior CGP effects on mechanical and microstructural properties of friction stir processed pure copper. The main achievement of this research was that the specimens which experienced prior CGP have high strength base metal along with high strength and ductility, while FSPed specimens without prior CGP suffer from the weak base metal. Some of the main achievements are presented below:

1- Performing FSP on the CGPed copper considerably decreases the grain size (from 50 to 5 μm), and upon application of higher FSP passes on the same

specimen; slight increase in the grain size was observed. Applying higher FSP passes on the annealed copper alternatively reduces the grain size.

2- Calculated results exhibited that CGP increases the dislocation density in the annealed copper more than one order of magnitude, whereas application of FSP leads to a reduction of dislocation density.
3- FSP increases the dislocation density of the annealed copper, but this increase is not comparable with those that of pre-CGPed specimens.
4- The yield stresses of processed specimens show remarkable improvements compared with the annealed ones. FSP reduces the yield stress of CGPed specimens as a result of the existence of higher heat input.
5- FSP leads to simultaneous improvement of ultimate tensile strength and strain values of the CGPed and annealed specimens.
6- Microhardness values of the processed specimens were well correlated with their dislocation density values and order of heat input as the 1C and 1C-2F specimens show the highest and lowest microhardness values, respectively.

References

[1] P.G. Sanders, J.A. Eastman, J.R. Weertman: Acta mater, 45 (1997) 4019-4025.
[2] V. Rajinikanth, A. Gaurav, N. Narasaiah, K. Venkateswarlu: Mater Lett, 62 (2008) 301–304.
[3] Y. Iwahashi, J. Wang, Z. Horita, M. Nemoto: Scr Mater, Scr Mater, 35 (1996)143-146.
[4] A. Dodangeh, M. Kazeminezhad, H. Aashuri: Mater Sci Eng A, 558 (2012) 371–376.
[5] A. Azushima, R. Kopp, A. Korhonen, D.Y. Yang, F. Micari, G.D. Lahoti, P. Groche, J. Yanagimoto, N. Tsuji, A. Rosochowski, A. Yanagida: Manu Technol, 57(2008) 716–735.
[6] R.K. Islamgaliev, N.F. Yunusova, I.N. Sabirov, A.V. Sergueeva, R.Z. Valiev: Mater Sci Eng A, 319–321(2001)877–881.
[7] Y. Miyajima, M. Mitsuhara, S. Hata, H. Nakashima, N. Tsuji: Mater Sci Eng A, 528 (2010) 776–779.
[8] M. Furukawa, Z. Horita, M. Nemoto, T.G. Langdon: Mater Sci Eng A, 324 (2002) 82–89.
[9] P. Leo, E. Cerri, P.P. De-Marco, H.J. Roven: J Mater Process Technol, 182 (2007) 207–214.
[10] Y.T. Zhu, T.C. Lowe, T.G. Langdon: Scr Mater, 51 (2004) 825–830.
[11] F. Khodabakhshi, M. Kazeminezhad: Mater Des, 32 (2011) 3280–3286.
[12] D.H. Shina, J-J. Park, Y-S. Kim, K-T. Park: Mater Sci Eng A, 328, (2002) 98–103.
[13] S.C. Yoon, A. Krishnaiah, U. Chakkingal, H.S. Kim: Comput Mater Sci, 43 (2008) 641–645.
[14] J.W. Lee, J.J. Park: J Mater Process Technol, 130 (2002) 208–213.
[15] L. Lu, Y. Shen, X. Chen, L. Qian, K. Lu: Science, 304 (2004) 422-425.
[16] P. Xue, B.L. Xiao, Z.Y. Ma: Mater Sci Eng A, 532 (2012) 106–110.
[17] R.S. Mishra, Z.Y. Ma: Mater Sci Eng R, 50 (2005) 1–78.
[18] J-Q. Su, T.W. Nelson, T.R. Mcnelley, R.S. Mishra: Mater Sci Eng A, 528 (2011) 5458–5464.
[19] M. Barmouz, M- K. Besharati Giv: Composites: Part A, 42 (2011) 1445–1453.

[20] M. Barmouz, K. Abrinia, J. Khosravi: Mater Sci Eng A, 559 (2013) 917–919.
[21] M. Sarkari Khorrami, M. Kazeminezhad, A.H. Kokabi: Mater Des, 40 (2012)364–372.
[22] I. Topic, HW. Höppel, M. Göken: Mater Sci and Eng A, 503 (2009)163–166.
[23] Y. Sun, H. Fujii, Y. Takada, N.Tsuji, K. Nakata, K. Nogi: Mater Sci Eng A, 527 (2009) 317–321.
[24] A. Sajadi, M. Ebrahimi, F. Djavanroodi: Mater Sci Eng A, 552 (2012) 97– 103.
[25] F. Khakbaz, M. Kazeminezhad: Mater Sci Eng A, 532 (2012) 26–30.
[26] M. Barmouz, M-K. Besharati Givi, J. Seyfi: Mater Charact, 62 (2011) 108–117.
[27] W-B. Lee, S-B. Jung: Mater Lett, 58 (2004) 1041–1046.
[28] M. Barmouz, M-k. Besharati Givi, J. Jafari: J Mater Eng Perform, 23 (2014) 101–107.
[29] H. Khodaverdizadeh, A. Mahmoudi, A. Heidarzadeh, E. Nazari: Mater Des, 35 (2012) 330–334.
[30] E. Rafizadeh, A. Mani, M. Kazeminezhad: Mater Sci Eng A, 515 (2009)162–168.
[31] J-C. Lee, HK. Seok, JH. Han, YH. Chung: Mater Res Bull, 36 (2001) 997–1004.
[32] H. Hahn, P. Mondal, K.A: Nanostruct Mater, 9 (1997) 603-606.
[33] D K-W: Mater Sci Eng, 113 (1989)1–41.
[34] RJ. Amodeo, NM. Ghoniem: Physics Review B, 41 (1990) 6968-6976.
[35] D.P. Field, B.W. True, T.M. Lillo, J.E. Flinn: Mater Sci Eng A, 372 (2004)173–179.